

# Isobutane/2-butene alkylation on dealuminated H EMT and H FAU

Michael Stöcker<sup>1</sup>, Helle Mostad, Arne Karlsson, Hanne Junggreen and Britt Hustad

*Department of Hydrocarbon Process Chemistry, SINTEF Oslo, POBox 124 Blindern, N-0314 Oslo, Norway*

Received 30 November 1995; accepted 29 March 1996

The alkylation of isobutane with 2-butene on dealuminated hexagonal H EMT and dealuminated cubic faujasite H FAU with Si/Al ratios of 5–6 was studied at 80°C and compared with results obtained for the as-synthesized and calcined parent material with Si/Al ratios of 3.5. In both cases, the dealuminated samples favour an improved profile with respect to the alkylate yield and selectivity after 3 h reaction time, with dealuminated H EMT as the superior system. The alkylate composition consisted of 76% and about 70% C<sub>8</sub> paraffins for dealuminated H EMT and dealuminated H FAU, respectively. Within the C<sub>8</sub> fractions the three trimethylpentanes (TMP) 2,3,3-, 2,3,4- and 2,2,4-TMP were the dominating product compounds in all tests, whereas a higher content of dimethylhexanes (DMH) was observed for the H FAUs, both dealuminated and parent material. However, among the four trimethylpentanes (2,2,3-, 2,2,4-, 2,3,3- and 2,3,4-TMP) usually the 2,3,3-TMP and 2,3,4-TMP were the main compounds formed, at least for the dealuminated samples. Oligomerization was suppressed by using the dealuminated samples, however, increasing amounts of C<sub>8</sub> olefins after about one half of the monitored reaction time was observed for the H FAUs. By contrast, the H EMTs exhibited much less formation of C<sub>8</sub> olefins (and on a constant level) even after 300 min reaction time. The deactivated samples showed mainly formation of paraffinic coke.

**Keywords:** dealuminated hexagonal faujasite (EMT); dealuminated cubic faujasite (FAU); isobutane/2-butene alkylation

## 1. Introduction

Isobutane/butene alkylation is a well known refinery technology for obtaining high octane number gasoline besides the FCC process. The present technology applies either hydrofluoric acid or concentrated sulfuric acid in a liquid phase reaction, leading to a number of problems such as separation procedures, environmental constraints, corrosion etc. Therefore, the search for alternative, heterogeneous catalysts, substituting the present HF or H<sub>2</sub>SO<sub>4</sub> based homogeneous systems, is still going on, with zeolites among the most promising catalysts [1,2]. In a previous paper we reported the H EMT (Si/Al = 3.5) showing an alkylate product distribution pattern (C<sub>8</sub> paraffins) comparable to those obtained by HF or H<sub>2</sub>SO<sub>4</sub> catalyzed reactions [3]. However, all the heterogeneous acid catalysts reported so far (including the zeolites) deactivate rapidly, mainly due to the loss of hydride transfer capacity leading to the formation of oligomerisate instead of alkylate.

In the case of zeolites, cubic faujasites (X and Y zeolites) have so far been the most investigated systems. Common for most of these large-pore zeolites is the fact, that they can adsorb TMPs, which are the most desired gasoline compounds in the alkylate formed.

In the present study we investigate the potential of the dealuminated hexagonal faujasite (H EMT) and dealuminated cubic faujasite (H FAU) as catalysts in the alkylation of isobutane with 2-butene, with emphasis on the C<sub>8</sub> composition, the trimethylpentanes (TMP) distri-

bution (due to the high octane numbers needed for high quality gasoline), dimethylhexanes (DMH), and C<sub>8</sub> olefins formation.

## 2. Experimental

Syntheses of parent H EMT and H FAU (Si/Al ratios of 3.5) were performed according to the (slightly modified) procedures described by Delprato et al. [4], using 18-crown-6 ether and 15-crown-5 ether as templates, respectively.

EMT was synthesized in a 250 ml Teflon bottle containing 90.6 g Ludox LS and 65.6 g of a sodium aluminate solution, which was stirred with an ultrastirrer for 1 min. 12.4 g 18-crown-6 ether crystals were added and the final gel was again stirred for 1 min. The molar ratio of the gel composition was calculated to 0.3 Al<sub>2</sub>O<sub>3</sub> : 3.0 SiO<sub>2</sub> : 0.8 Na<sub>2</sub>O : 0.3 18-crown-6 : 43.0 H<sub>2</sub>O. The bottle content was then aged at room temperature for 18 h. before placement at 110°C for four weeks. Pure crystals of EMT were then obtained after filtration, washing and drying.

FAU was synthesized in a 125 ml Teflon bottle containing 55.1 g Ludox LS and 38.1 g of a sodium aluminate solution by shaking vigorously for 1 min. 6.1 g 15-crown-5 ether were added and the final gel was again shaken for 1 min. The molar ratio of the gel composition was calculated to 0.3 Al<sub>2</sub>O<sub>3</sub> : 2.9 SiO<sub>2</sub> : 0.7 Na<sub>2</sub>O : 0.3 15-crown-5 : 40.0 H<sub>2</sub>O. The bottle content was then aged at room temperature for 18 h before placement at 100°C for two weeks. Pure crystals of FAU were then obtained after filtration, washing and drying.

<sup>1</sup> To whom correspondence should be addressed.

The H-forms of the faujasites were obtained by ion-exchange of the parent material with 2 M  $\text{NH}_4\text{NO}_3$  solutions at 70°C (three times for 3 h each) and calcination at 540°C for 5 h in air (flow rate of 100 ml/min).

Dealumination was carried out by treatment of the parent material with  $(\text{NH}_4)_2\text{SiF}_6$  following the recipe of Léger et al. [5]: 15 g ammonium nitrate ion-exchanged parent material (EMT or FAU) was dispersed in 1350 ml 0.8 M ammonium acetate with magnetic stirring. The dispersion was heated to 75°C. 78 ml 0.45 M  $(\text{NH}_4)_2\text{SiF}_6$  solution was added dropwise over a period of 1.5 h. The mixture was then stirred for another 1.5 h at 75°C. The dealuminated sample was filtered, washed five times with hot water and dried at 100°C overnight.

XRD diffractograms were recorded with  $\text{Cu K}\alpha$ -rays within the angle ratio  $2\theta = 5\text{--}90^\circ$  on an X-ray diffractometer Philips PW 1730 equipped with a Siemens type F monochromator.

The MAS NMR spectra were recorded on a Varian VXR 300 S WB NMR spectrometer equipped with 7 mm zirconia rotors (except for the dealuminated H FAU). Conditions for the  $^{29}\text{Si}$  MAS NMR spectra: resonance frequency: 59.6 MHz, sweep width: 14000 Hz, pulse width: 8  $\mu\text{s}$ , repetition time: 5 s, number of scans: min. 1000, MAS spinning speed: 4.5–5 kHz. Conditions for the  $^{27}\text{Al}$  MAS NMR spectra: resonance frequency: 78.2 MHz, sweep width: 50000 Hz, pulse width: 0.5  $\mu\text{s}$ , repetition time: 2 s, number of scans: min. 1000, MAS spinning speed: 5–5.5 kHz. Conditions for the  $^{13}\text{C}$  CP/MAS NMR spectra: resonance frequency: 75.4 MHz, sweep width: 50000 Hz, pulse width: 8  $\mu\text{s}$ , repetition time: 10 s, contact time: 3 ms, number of scans: min. 2000, MAS spinning speed: 4.5–5 kHz. The MAS NMR spectra of the dealuminated H FAU were recorded on a Bruker MSL 400 NMR spectrometer under the following conditions:  $^{29}\text{Si}$  MAS NMR: resonance frequency: 79.5 MHz, sweep width: 18000 Hz, pulse width: 2  $\mu\text{s}$ , repetition time: 20 s, number of scans 2400, MAS spinning speed: 4 kHz. Conditions for the  $^{27}\text{Al}$  MAS NMR spectrum: resonance frequency: 104.3 MHz, sweep width: 30000 Hz, pulse width: 0.8  $\mu\text{s}$ , repetition time 1 s, number of scans: 2814, MAS spinning speed: 9.8 kHz.

TPD measurements were carried out on an AMI-1 instrument from Altamira Instruments Inc. which was controlled by a Hyundai PC-AT. TPD of ammonia was performed according to the following procedure (200 mg catalyst, particle size 35–70 mesh): Pretreatment with 30 ml/min He flow up to 600°C (samples calcined at 540°C). Saturation of the catalyst surface with 30 ml/min 10% ammonia in a He flow at 200°C. TPD with 30 ml/min He flow using the following temperature profile: 200°C in 30 min, increasing the temperature from 200 to 600°C with 20°C/min and then standby for 15 min at 600°C. Cooling to 100°C and calibration of the TCD by sending seven pulses of 5 ml ammonia.

IR spectra were recorded on a Perkin Elmer model 2000 FT-IR spectrometer equipped with a MCT detec-

tor and using a transmission in situ reactor cell (ISRI). The samples were pressed into self-supporting disks ( $d = 1.8$  mm, mass 7–10 mg/cm<sup>2</sup>) and investigated in the temperature range of 25–550°C. The spectra were recorded during heating/activation in vacuo and under subsequent pyridine adsorption. Pyridine was allowed into the cell at temperatures below 100°C. The sample was then heated at 150°C for about 30 min in vacuo in order to remove physisorbed pyridine, and subsequently the IR spectra were registered after heating to increasing temperatures. All spectra were recorded at a sample temperature of 150°C. Sample weights were corrected according to their weight loss measured by TGA.

SEM micrographs were obtained using a Jeol JSM-840 microscope equipped with a back-scattered electron detector.

One-point BET determinations were performed with a Quantachrome Monosorb and pore volume measurements were carried out applying a Carlo Erba Sorptomatic 1800.

Isobutane/2-butene reactor testing was performed in a liquid-phase 300 ml stirred semibatch autoclave, equipped with a cooled pulsation-free displacement pump for charging the reactants. 5.3 g of the calcined catalyst (540°C/5 h in air, the moisture content was checked by TGA) was placed in the reactor and dried further (200°C/2 h) before adding the isobutane. The mixture was then heated to 80°C under nitrogen pressure. 2-butene was charged slowly until the molar ratio of isobutane/2-butene reached 10 : 1. The alkylation reaction was carried out with a WHSV of 1.2 h<sup>-1</sup> (for 2-butene) and a stirring speed of 360 rpm. Differential one-phase liquid samples were taken regularly and analyzed by GC (capillary column from Hewlett Packard HP PNA 50 m×0.22 mm, i.d. 0.5  $\mu\text{m}$ , methylsilicone gum fused silica). Samples were thoroughly sucked to fill the transparent tubes, and injected directly into the GC for light component analysis. Excess liquid was collected in ice-cooled traps for off-line GC analysis (same column) of heavier products and separation of olefins. The amount of 2,3-dimethylbutane was used to standardize the product distribution from both GC-runs.

### 3. Results and discussion

The pure crystals of parent H EMT were checked by XRD (pure phase of EMT, 100% crystallinity, defined as percent of the intensity of the 4.35 Å reflection of a reference batch EMT or FAU, respectively), microprobe (bulk Si/Al ratio = 3.5),  $^{29}\text{Si}$  MAS NMR (framework Si/Al ratio = 3.5),  $^{27}\text{Al}$  MAS NMR (small amount of octahedrally coordinated aluminium besides mainly tetrahedrally coordinated aluminium), BET (surface area of 682 m<sup>2</sup>/g), SEM (hexagonal crystals of a mean size of about 3  $\mu\text{m}$ ) and porosity measurements (pore volume of 0.30 ml/g). The pure crystals of parent H FAU were

checked by XRD (pure phase of FAU, 95% crystallinity), microprobe (bulk Si/Al ratio = 3.8),  $^{29}\text{Si}$  MAS NMR (framework Si/Al ratio = 3.6),  $^{27}\text{Al}$  MAS NMR (only tetrahedrally coordinated aluminium), BET (surface area of 743  $\text{m}^2/\text{g}$ ), SEM (cubic crystals of a mean size of about 3  $\mu\text{m}$ ) and porosity measurements (pore volume of 0.34  $\text{ml/g}$ ).

The pure crystals of dealuminated H EMT were checked by XRD (pure phase of EMT, 76% crystallinity), microprobe (bulk Si/Al ratio = 6.1),  $^{29}\text{Si}$  MAS NMR (framework Si/Al ratio = 6.1),  $^{27}\text{Al}$  MAS NMR (very small amount of octahedrally coordinated aluminium besides mainly tetrahedrally coordinated aluminium), BET (surface area of 675  $\text{m}^2/\text{g}$ ), SEM (hexagonal crystals of a mean size of about 3  $\mu\text{m}$ ) and porosity measurements (pore volume of 0.27  $\text{ml/g}$ ). The pure crystals of dealuminated H FAU were checked by XRD (pure phase of FAU, 79% crystallinity), microprobe (bulk Si/Al ratio = 5.0),  $^{29}\text{Si}$  MAS NMR (framework Si/Al ratio = 7.6),  $^{27}\text{Al}$  MAS NMR (certain amount of octahedrally coordinated aluminium besides mainly tetrahedrally coordinated aluminium) which explains the difference between the bulk and framework Si/Al ratios), BET (surface area of 712  $\text{m}^2/\text{g}$ ), SEM (cubic crystals of a mean size of about 3  $\mu\text{m}$ ) and porosity measurements (pore volume of 0.33  $\text{ml/g}$ ).

Table 1 summarizes the activity after running the isobutane/2-butene alkylation over a period of 180 min reaction time for H EMT and H FAU, both parent and dealuminated samples. The conversion of 2-butene was

determined, concluding with an almost complete conversion of 2-butene applying the two H EMTs (especially for the dealuminated sample), whereas the conversions for the cubic faujasites H FAUs arrived at certain lower levels (see table 1 and fig. 1). One should emphasize, that our comparisons in table 1 are based on different conversion levels for H EMT and H FAU. The  $\text{C}_8$  paraffins are, however, the dominating fractions, with a content of more than 76% of the product distribution for the H EMTs and about 64–69% for the H FAUs. The alkylate yields (defined as g  $\text{C}_5$ – $\text{C}_8$  paraffins per g dry catalyst) were calculated to 3.8 and 4.8 for the H EMTs and to 1.4 and 2.1 for the H FAUs, respectively. The selectivities, defined as g  $\text{C}_5$ – $\text{C}_8$  paraffins per g 2-butene converted were determined to 1.8 and 2.0 for the H EMTs and to 1.0 and 1.3 for the H FAUs, respectively.

The total 2-butene turnover numbers (TON, moles of 2-butene converted per mole acid sites) for the catalysts are plotted in fig. 1, together with the values for the maximum possible turnover numbers calculated from the theoretical number of acid sites (based on framework chemical analysis and taking into account the remaining Na content). During the feeding time for 2-butene (120 min) the actual TON are slightly less than the theoretical values. The EMT catalysts convert almost all added 2-butene during the first 120 min of reaction, with significant larger TON for the dealuminated EMT than for the parent material. After 120 min, the 2-butene turnover was observed to be nearly con-

Table 1

Isobutane/2-butene alkylation activity obtained at 80°C on the parent (H EMT, H FAU, Si/Al = about 3.5) and dealuminated faujasites (H EMT, H FAU, Si/Al = 5–6) after 3 h reaction time in a slurry reactor

	Catalyst			
	parent H EMT	deal. H EMT	parent H FAU	deal. H FAU
2-butene conversion (%)	88	98	66	67
alkylate yield <sup>a</sup>	3.8	4.8	1.4	2.1
selectivity <sup>b</sup>	1.8	2.0	1.0	1.3
product distribution (norm %)				
$\text{C}_5$ – $\text{C}_7$ paraffins	9.6	7.6	23.0	18.1
$\text{C}_8$ paraffins	81.9	76.4	64.4	69.3
$\text{C}_8$ olefins	0.5	none	3.1	2.9
$\text{C}_{9+}$ paraffins, olefins	7.9	15.8	9.3	9.8
isooctane distribution (norm %)				
2,3-DMH	4.9	6.1	4.8	6.2
2,4-DMH	1.4	2.4	4.0	4.2
3,4-DMH	2.3	2.1	3.6	2.7
2,2,3-TMP/2,5-DMH	14.7	7.9	7.1	6.4
2,2,4-TMP	24.4	18.3	26.9	24.4
2,3,3-TMP	29.5	34.1	29.1	29.8
2,3,4-TMP	22.1	28.5	24.2	26.3
isooctenes in $\text{C}_8$ products (norm%)	0.6	none	4.6	4.0

<sup>a</sup> Alkylate yield: g  $\text{C}_5$ – $\text{C}_8$  paraffins / g dry catalyst.

<sup>b</sup> Selectivity: g  $\text{C}_5$ – $\text{C}_8$  paraffins / g 2-butene converted.

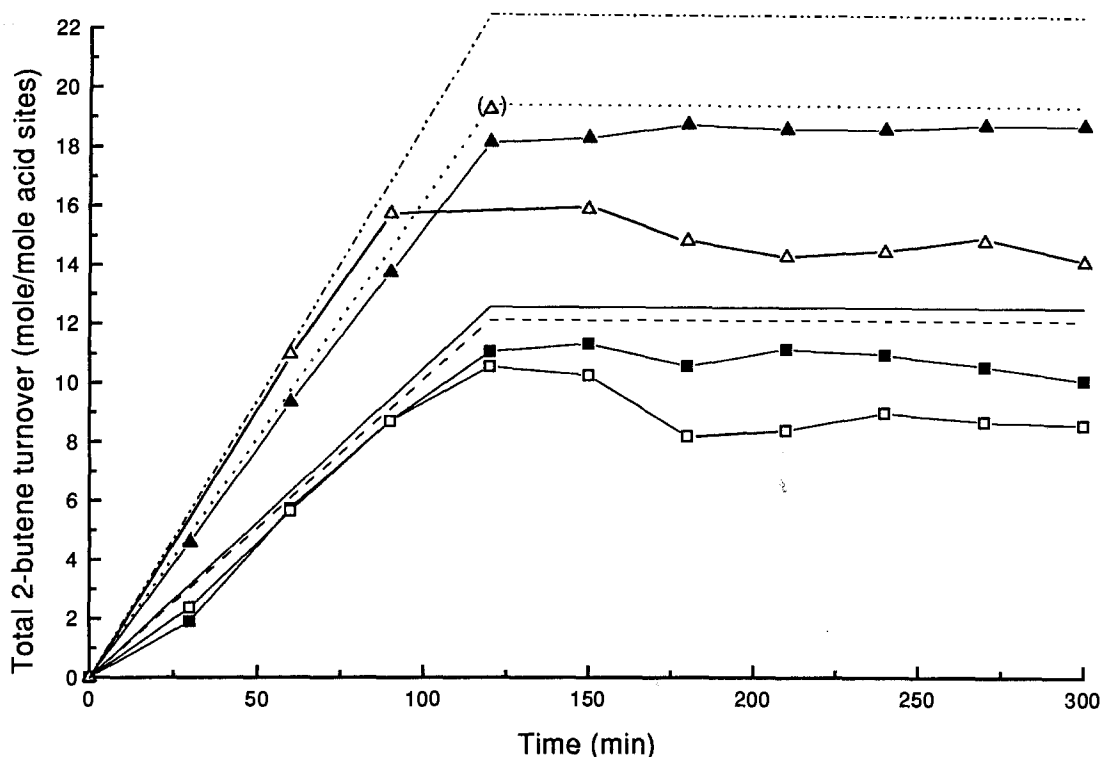


Fig. 1. Conversion of 2-butene measured as total 2-butene turnover number (TON) with time of reaction for the parent HFAU (□), dealuminated HFAU (△), parent HEMT (■) and dealuminated HEMT (▲). The maximum possible turnover numbers calculated from the theoretical number of acid sites are included for the parent HFAU (—), dealuminated HFAU (---), parent HEMT (— · —) and dealuminated HEMT (···).

stant for both HEMT systems. The FAU systems did not convert all added 2-butene during the first 120 min of reaction and were not able to convert the rest of 2-butene in the reaction mixture during the next 180 min due to deactivation of the active acid sites by oligomerization. The apparent decrease in TON after 120 min for the FAU catalysts is probably due to an artificial small measured amount of 2-butene in the reaction mixture after the 2-butene feeding was terminated.

The normalized distributions of the  $C_8$  paraffins fractions after 180 min reaction time are shown in table 1, too. The HEMTs exhibited less amounts of DMHs compared to the HFAUs. Among the four investigated catalysts, the distribution of the four TMPs is at about the same level, however, a few significant deviations are registered. Within the four TMPs, the isomers 2,3,3-TMP and 2,3,4-TMP were the dominating ones (at least for the dealuminated samples), which is in contradiction to the equilibrium distribution of the TMP isomers at 80°C and to results obtained by application of macroporous systems, like resins or aluminosilicate [2,6,7]. Even for Y zeolite, a similar behaviour was observed [8]. At that temperature, the 2,2,4-TMP should be the superior isomer, whereas this compound is only formed to less extent (compared to both 2,3,3- and 2,3,4-TMP) applying our dealuminated faujasites. 2,2,3-TMP has been reported as the less formed isomer [7,8], which is in line with our findings. However, according to the thermodynamic equilibrium concentration at this temperature,

this isomer should be produced to a larger extent [2]. Obviously, the primarily formed secondary 2,2,3-TMP<sup>+</sup> cation undergoes a rapid isomerization due to successive hydride and methyl shifts [8]. The discrepancies related to the preferred formation of 2,3,3- and 2,3,4-TMP and to the less formed 2,2,3-TMP by use of dealuminated hexagonal and cubic faujasites demonstrates obviously a kinetically favoured production of 2,3,3- and 2,3,4-TMP. This could be explained by admitting that the hydride transfer to a tertiary carbenium ion is infinitely faster than to a secondary carbenium ion. In agreement with this, the TMPs which are the most favoured, are those of which only tertiary carbenium ions exist (2,3,4-TMP) or can be formed through methyl shift (2,3,3-TMP) [8]. In addition, a shape-selective effect of those molecular sieves might control the formation of these TMPs, compared to steric less restricted solid catalysts or homogeneous systems following a TMP product pattern corresponding to the thermodynamic equilibrium concentrations.

The composition of the four TMPs during the runs changed only slightly (up to 300 min reaction time). An increase for 2,2,3-TMP and slight decreases for 2,3,3- and 2,3,4-TMP were observed for the parent HEMT, whereas for the parent HFAU a small decrease was observed for 2,3,3-TMP. For the dealuminated HFAU a certain decrease was registered for 2,2,4-TMP (see fig. 2).

The higher degree of  $C_8$  paraffin formation in the

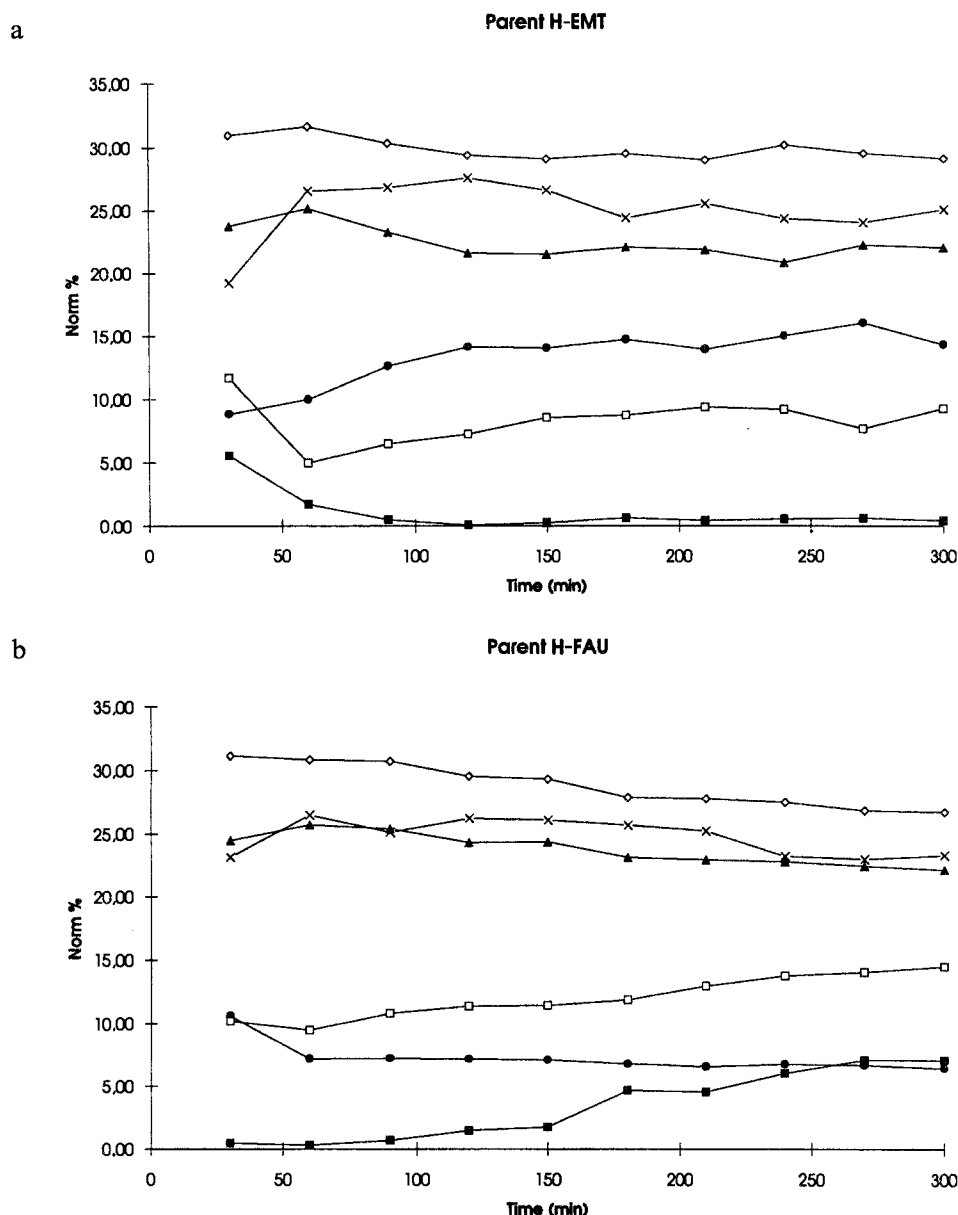


Fig. 2 Normalized distribution of the formed DMHs (sum, except 2,5-DMH), TMPs and C<sub>8</sub> olefins (in %) with time of reaction in the isobutane/2-butene alkylation over (a) parent H EMT, (b) parent H FAU, (c) dealuminated H EMT and (d) dealuminated H FAU (temperature: 80°C, WHSV (for 2-butene): 1.2 h<sup>-1</sup>, stirring speed: 360 rpm). (×) 2,2,4-TMP; (●) 2,2,3-TMP (includes 2,5-DMH); (▲) 2,3,4-TMP; (◇) 2,3,3-TMP; (■) C<sub>8</sub>=; (□) DMH.

alkylate of the two H EMTs can be traced back to the slightly larger size of the second type of supercage in the structure of the hexagonal faujasite, compared to the uniform size of supercages in the cubic FAU system and to the higher conversion of 2-butene. Furthermore, with respect to the C<sub>5</sub>–C<sub>8</sub> alkylate yields and selectivities, again the two H EMTs are the superior catalysts, which favour, in addition, slightly less formation of undesired DMH.

The formation of DMHs (except for 2,5-DMH due to coeluting peaks in the gas-chromatogramme) during the course of the reaction (60–300 min) is up to 11

norm% of the C<sub>8</sub> distribution for both H EMT samples on a constant level, whereas up to 14 norm% was observed for the H FAU samples. Only DMHs having at least one tertiary carbon atom are formed. Concerning the formation of C<sub>8</sub> olefins, the superior role of the two H EMT samples is clearly demonstrated with very low amount of C<sub>8</sub> olefins compared to the two H FAUs (see table 1 and fig. 2).

The H FAU systems showed a tendency to oligomerize followed by the formation of cracking products in the C<sub>5</sub>–C<sub>7</sub> paraffin range, whereas this phenomenon was observed to a much smaller extent for the H EMT cat-

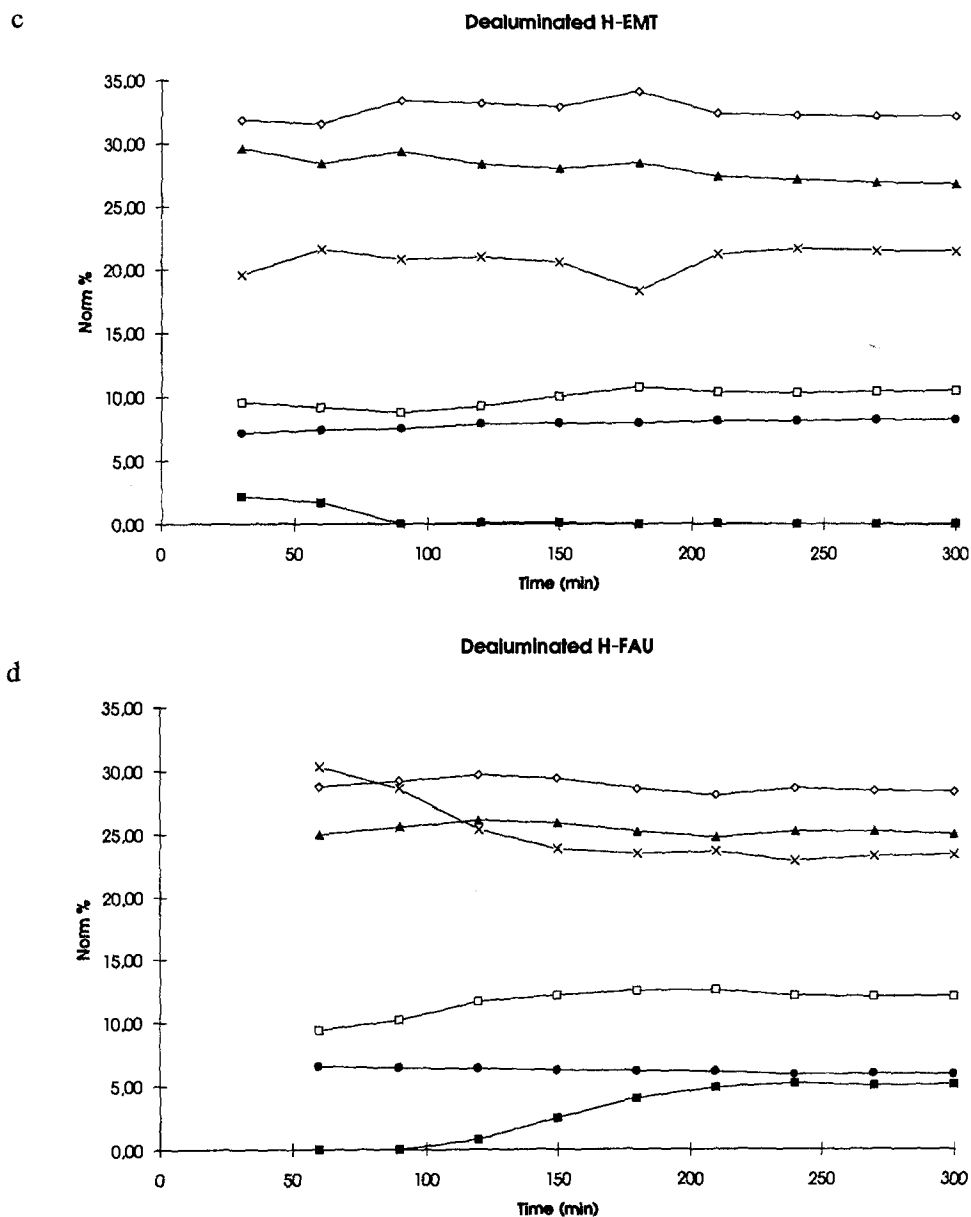


Fig. 2. (Continued.)

alysts. Concerning the formation of  $C_{9+}$  paraffins and olefins, the level was about the same for all catalysts, except for the dealuminated H EMT, which revealed a large amount of those products.

The nature, number and strength of the acid sites in the investigated catalysts are important with respect to the result interpretation. Our acidity measurements (TPD of ammonia and IR spectroscopy) arrived at the following results: The amount of acid sites measured by TPD of ammonia was about 2.1 mmol  $NH_3$ /g catalyst for the parent H EMT system, which is in line with findings by Lohse et al. [9], and about 1.7 mmol  $NH_3$ /g catalyst for the parent H FAU system. It has been reported in the literature that the stability of the hydroxyl groups is strongly influenced by the pretreatment temperature and varies for the different structures [10]. Our observation of a smaller amount of hydroxyl groups in the par-

ent H FAU than in the parent H EMT (both samples calcined at 540°C) is in agreement with the lower observed stability of the hydroxyl groups of H Y than those of the parent H EMT (pretreated at the same temperature) [10]. The maximum peak temperatures were measured to be 310–320°C and 400–430°C for the parent materials of both catalyst groups. A pronounced increase in acid strength of the remaining sites was observed for both dealuminated samples compared to the parent systems, by measuring a shift of the high temperature peak from 410 to 450°C. Thus, the TPD measurements of the dealuminated samples confirm an increase in the strength of the remaining acid sites. This increase may contribute to the observed improvement of the alkylate yield and selectivity of both the dealuminated H EMT and H FAU samples as compared with the H forms of the parent materials.

IR spectra of the parent H FAU showed strong bands at  $3632\text{ cm}^{-1}$  (high frequency hydroxyl, HFOH) and  $3545\text{ cm}^{-1}$  (low frequency hydroxyl, LFOH) for OH groups in the supercages and sodalite cages, respectively. A weak band at  $3734\text{ cm}^{-1}$  is possibly due to silanol groups in hydroxyl nests. Dealumination of the H FAU sample led to new bands in the spectrum at  $3663$ ,  $3598$  and  $3558\text{ cm}^{-1}$ , while the HFOH and LFOH bands shifted slightly to  $3630$  and  $3538\text{ cm}^{-1}$ , respectively. Frequencies near  $3598$  and  $3558\text{ cm}^{-1}$  have been assigned to OH groups in the supercages and sodalite cages, respectively. They shifted obviously from the original HFOH and LFOH wavenumbers as a result of an interaction with Al cationic species localized in the sodalite cages [11]. The  $3663\text{ cm}^{-1}$  band were assigned to a different type of extra-framework species [11].

The IR spectra of the parent H EMT and dealuminated H EMT are quite similar. The HFOH bands are located at  $3627\text{ cm}^{-1}$  for both samples, while the LFOH bands have frequencies at  $3545\text{ cm}^{-1}$  in the parent H EMT and at  $3550\text{ cm}^{-1}$  in the dealuminated H EMT. No extra bands, or modifications in the band profiles can be observed as a result of the dealumination, pointing to Al removal without generation of extra-framework aluminium species. Weak bands at  $3734\text{ cm}^{-1}$  are present in the spectra of the H EMT samples, too.

In the parent H FAU, pyridine interacts almost completely with the HFOH and with most of the LFOH at  $150^\circ\text{C}$ . At elevated temperatures the LFOH are liberated first (below  $450^\circ\text{C}$ ) while some of the HFOH are still interacting with pyridine at  $550^\circ\text{C}$ . In the more complex hydroxyl "massif" of dealuminated H FAU, almost complete interaction seems to occur for all OH groups except those at  $3598\text{ cm}^{-1}$  for which only a small fraction interacts. Increasing the temperature leads to the liberation of OH groups in approximately equal proportion, most noticeable in the  $400\text{--}550^\circ\text{C}$  temperature range. As already mentioned, an exception is the small number of OH with a frequency at  $3598\text{ cm}^{-1}$ , for which interaction with pyridine appear to remain almost unaltered even at  $550^\circ\text{C}$ .

For the two H EMT samples, complete interaction of pyridine can be observed for both the HF and LF hydroxyl groups at  $150^\circ\text{C}$ . Further increase of the temperature reveals an almost identical desorption pattern of pyridine: the LFOH are gradually liberated, while a fairly large number of the HFOH interacts with pyridine even at  $550^\circ\text{C}$ .

Spectra of pyridine adsorbed on the samples at temperatures from  $150$  to  $550^\circ\text{C}$  were recorded in the range between  $1400$  and  $1700\text{ cm}^{-1}$ , too. Integrated absorbances for the Brønsted bands at about  $1540\text{ cm}^{-1}$  and the Lewis bands at about  $1450\text{ cm}^{-1}$  were converted to concentrations of Brønsted and Lewis acid sites (mmol/g catalyst) using molar extinction coefficients from the literature [12] and plotted as a function of the temperature for all the investigated samples in fig. 3. These

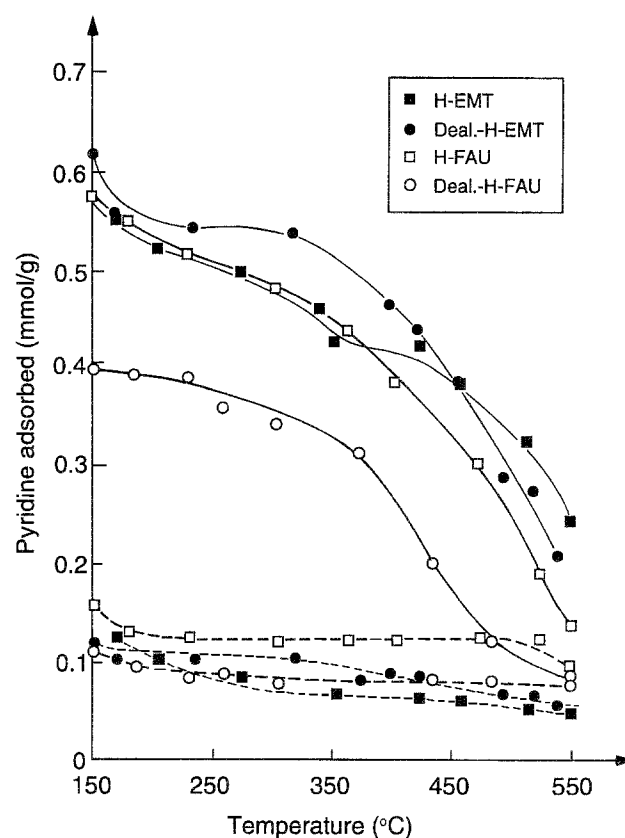


Fig. 3. Concentrations of Brønsted (solid lines) and Lewis acid sites (dashed lines) in mmol/g catalyst vs. temperature based on IR spectra of adsorbed pyridine for parent H EMT (■), dealuminated H EMT (●), parent H FAU (□) and dealuminated H FAU (○).

curves should reflect both the total concentrations of acid sites accessible to pyridine, and the distribution of these acid sites with respect to acid site strengths. The concentration of Brønsted acid sites is always significantly higher than the concentration of Lewis acid sites. However, for all samples the concentrations of Brønsted acid sites derived at  $150^\circ\text{C}$  are considerably lower than the theoretical values given by the Si/Al ratios measured for the samples. Recently, maximum amounts of pyridine adsorbed in both H FAU and H EMT samples were reported as approximately  $1.2\text{ mmol/g catalyst}$  [13]. Consequently, the number of pyridine indicated for our samples should reflect the actual number of acid sites capable for interaction. A decrease in the number of hydroxyls in the samples after calcination at  $540^\circ\text{C}$  seems likely [10], and assuming this, a lower thermal stability of the OH groups in the parent samples may be inferred, although in different degrees.

Corma et al. [14] used the ratio of pyridine adsorption at  $400^\circ\text{C}$  to that at  $250^\circ\text{C}$  as a measure of the relation between strong and weak acid sites in their samples. We obtained ratios of  $0.63$  and  $0.65$  for the parent and dealuminated H FAU samples, whereas the corresponding values for the parent and dealuminated H EMT samples were  $0.84$  and  $0.86$ , respectively. Additionally, all samples showed some pyridine adsorption at  $550^\circ\text{C}$ , indicat-

ing the presence of very strong acid sites in the samples. Our IR results are in general agreement with the TPD of ammonia investigations; however, they indicate quite different properties of the acid sites of the FAU and EMT samples. In addition to the high density of acid sites in general, the presence of strong acid sites and a high ratio of strong to weak acid sites have been reported to be important for the isobutane/2-butene alkylation reaction, taking into account a desired large alkylation activity and avoiding/suppressing the oligomerization [15]. Based on these arguments, our characterization of acid strength in the samples would rank the EMT samples as better catalysts than the FAUs for the alkylation reaction, in agreement with the observed test results.

The deactivated samples were checked by  $^{13}\text{C}$  CP/MAS NMR spectroscopy, and only non-aromatic coke components (mainly of paraffinic character like methyl groups connected to secondary carbon atoms (14 ppm),  $\text{CH}_2$  groups linked to methyl groups (22 ppm) and methyl groups at quaternary carbon atoms (29 ppm) besides small amounts of olefinic coke) were detected [16].

#### 4. Conclusion

In conclusion, the lower tendency of the H EMT samples to form DMHs and  $\text{C}_8$  olefins, as well as the high values of  $\text{C}_8$  paraffins, 2-butene conversion, alkylate yield and selectivity emphasize the superior behaviour of the H EMT samples as a promising isobutane/2-butene alkylation catalyst compared to H FAU. In addition, among the FAU samples, the dealuminated H FAU showed a significant better profile than the parent H FAU, but still less favourable than the EMT samples. These results are explained to a large extent by the differences measured for the acid strength distributions in the samples, showing a significantly larger ratio of strong-to-weak acid sites for the H EMTs investigated compared to the H FAU samples. The dealuminated H FAU may perform better than the parent material due to the presence of additional small numbers of very strong acid sites.

#### Acknowledgement

The authors are indebted to the Norwegian Research Council for financial support and to the European Commission for participation in the JOULE II programme.

#### References

- [1] V.N. Ipatieff and L. Schmerling, *Adv. Catal.* 1 (1948) 27; J. Weitkamp, *Acta Phys. Chem.* 31 (1985) 271; F.W. Kirsch, J.D. Potts and D.S. Barmby, *J. Catal.* 27 (1972) 142; J. Weitkamp, in: *Proc. 5th Int. Zeolite Conf.*, ed. L.V.C. Rees (Heyden, London, 1980) p. 858; J. Weitkamp, in: *Catalysis by Zeolites*, Studies in Surface Science and Catalysis, Vol. 5, eds. B. Imelik, C. Naccache, Y. Ben Taarit, J.C. Vedrine, G. Coudurier and H. Praliaud (Elsevier, Amsterdam, 1980) p. 65.
- [2] A. Corma and A. Martinez, *Catal. Rev. Sci. Eng.* 35 (1993) 483.
- [3] M. Stöcker, H. Mostad and T. Rørvik, *Catal. Lett.* 28 (1994) 203.
- [4] F. Delprato, L. Delmotte, J.L. Guth and L. Huve, *Zeolites* 10 (1990) 546.
- [5] Cl. Leger, B. Herreros, Ma. Hepp, J. Thoret, C. Potvin, Pp. Man and J. Fraissard, *J. Chim. Phys.* 91 (1994) 916.
- [6] W.E. Garwood and P.B. Venuto, *J. Catal.* 11 (1968) 175.
- [7] T.J. Huang and S. Yurchak, *Div. Petr. Chem. Am. Chem. Soc.* 22 (1977) 358.
- [8] F. Cardona, N.S. Gnep, M. Guisnet, G. Szabo and P. Nascimento, *Appl. Catal.* 128 (1995) 243.
- [9] U. Lohse, I. Pitsch, E. Schreier, B. Parltitz and K.-H. Schnabel, *Appl. Catal.* 129 (1995) 189.
- [10] B.L. Su and D. Barthomeuf, *Zeolites* 13 (1993) 626.
- [11] P.O. Fritz and J.H. Lundsford, *J. Catal.* 118 (1989) 85.
- [12] C.A. Emeis, *J. Catal.* 141 (1993) 347.
- [13] M.A. Makarova, K. Karim and J. Dwyer, *Microporous Mater.* 4 (1995) 243.
- [14] A. Corma, A. Martinez and C. Martinez, *J. Catal.* 146 (1994) 185.
- [15] A. Corma, A. Martinez and C. Martinez, *Catal. Lett.* 28 (1994) 187.
- [16] J. Weitkamp and S. Maixner, *Zeolites* 7 (1987) 6.